

Modeling Uncertainty in Photointerpreted Boundaries

G. Edwards and K.E. Lowell

Abstract

A model based on multiple photointerpretations for estimating local boundary uncertainty (or "fuzzy boundary width") between forest stands is developed and presented, using an artificial data set consisting of textured images of known class characteristics and locations. A fuzzy width estimator has been developed by breaking down the perceptual process of photointerpretation into two components: discrimination and variability. Discrimination consists of the ability of the photointerpreter to detect a difference in texture. Variability consists of the intrinsic spatial variability of the texture itself. A quantitative analysis of these effects led to a model relating the image construction parameters to the fuzzy boundary widths. The study is useful for examining the effect of context on boundary uncertainty and for suggesting how one might assess the uncertainty of boundaries extracted by more automated algorithms.

Introduction

The Importance of Uncertainty

GIS technology and techniques are increasingly used for forest management (Tomlinson, 1987). In Canada, as is typical elsewhere, digital forest maps are maintained using a variety of commercial platforms (Dick and Jordan, 1990). There are some significant difficulties, however, which are not directly addressed by the new technology, regardless of the particular technology adopted (e.g., raster versus vector).

One such difficulty relates to the fact that forest inventory continues to be based primarily on the interpretation of aerial photographs by one individual. Any two photointerpreters will not produce similar results (this is obvious from Figure 1), even when using the same material. A single interpreter may even provide significantly different results on two occasions (Nantel, 1993). Furthermore, photointerpretation accuracy is never very high (Biging *et al.*, 1992). Thus, it is difficult to evaluate changes in forest conditions over time, because the uncertainty in any forest map is high. It also means that it is difficult to reconcile two forest maps produced by the photointerpretation process (Figure 2). The availability of digital map products and GIS may worsen the problem, because more is being asked from map comparisons than when maps were only available on paper. In particular, when maps are incorporated into databases, the mapped representation of any given database object must be consistent from one time to the next. This is very hard to achieve with existing map representations, and is one of the reasons why the forest must be reinventoried every ten to fifteen years, and why the old inventory is usually *replaced*, rather than modified (Québec Ministry of Natural Resources, pers. comm.).

A second difficulty consists of the fragmentation of forest stands when time management is involved, as, for example, in the construction of space-time composites (Langran and Chrisman, 1988; Langran, 1992). As the forest changes, either naturally or because of exploitation, forest "polygons" (stands, etc.) must be broken into increasingly smaller regions. (Figure 2 provides a typical example of this.) Overlay processes in GIS also lead to a related fragmentation problem, with large numbers of very small polygons (so-called "sliver polygons") being generated when any two themes are overlaid (Goodchild, 1977; Dougenik, 1980). Existing techniques for "cleaning" up sliver polygons rely on merging them with their neighbors (Zhang and Tulip, 1990) or on moving segments (Dougenik, 1980), but only recently have such techniques become more sensitive to local context (Pulgar, 1991). Sliver polygons are, however, an indicator of spatial uncertainty and/or of gradual change. Assigning them to one or another of neighboring polygons is not always appropriate and, indeed, the "correct" handling of sliver polygons is a difficult problem. Moving boundary segments is also a complex task. The increasing number of themes managed by forestry GIS exacerbates these problems.

A possible solution to these problems is to represent each forest "boundary" as having a "fuzzy" width and to apply an appropriate, probability-like approach to obtain spatial operators which can be used to evaluate data consistency. Existing work on representing boundaries as having width (e.g., "epsilon" bands) includes that of Goodchild (1977), Chrisman (1982), Blakemore (1984), Chrisman and Lester (1991), Dunn *et al.* (1990), and Dutton (1992). In these treatments, however, a single width has been employed for all boundaries of a given map. We propose using a variable boundary width which depends on the two classes on each side of the boundary. In forestry, the boundary between a mature stand and a clear cut, for example, is relatively easy to find, whereas the boundary between two density classes may be relatively difficult to identify (Lowell *et al.*, 1992). If the width of these fuzzy boundaries corresponds to the real-world spatial uncertainty, then when two photointerpreted maps from different times are compared, one may be able to determine which boundaries are consistent from one map to the other, and which boundaries are new and hence represent real change. In addition, if appropriate probabilistic techniques of overlay can be developed, the intersection of the two maps will not be a great number of meaningless fragments, but will represent the real changes between the two maps.

In the epsilon-band technique, the band represents boundary error as a probability distribution function of pos-

Photogrammetric Engineering & Remote Sensing,
Vol. 62, No. 4, April 1996, pp. 337-391.

Chaire industrielle en géomatique appliquée à la foresterie,
Centre de recherche en géomatique, Pavillon Casault, Université Laval, Sainte-Foy, Québec G1K 7P4, Canada.

0099-1112/96/6204-377\$3.00/0

© 1996 American Society for Photogrammetry
and Remote Sensing

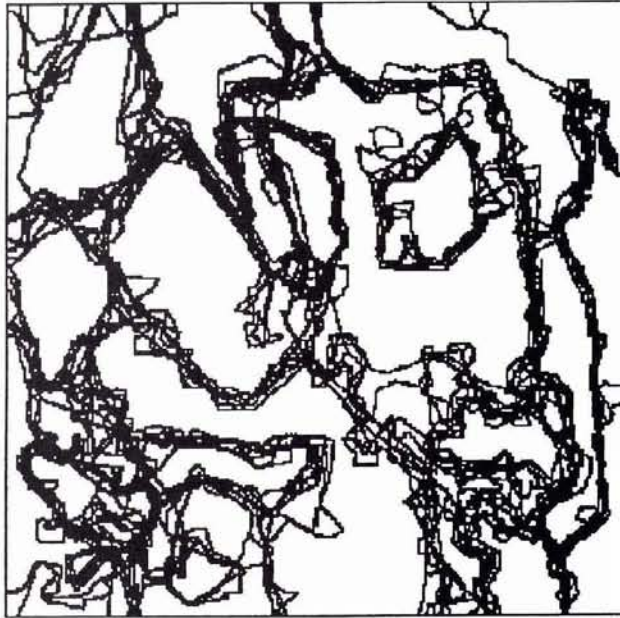


Figure 1. Nine interpretations of Image #1 (see Figure 3a).

gen (1991) identifies two schools of inquiry in studies of human visual processing, one initiated by Julesz (1962) and the other by Beck (1966). Julesz began by characterizing image texture in terms of global first- and second-order statistics, while Beck began by identifying individual features of "texture elements" and their spatial arrangement. Both lines of inquiry converged in the 1980s on a number of common elements (Beck *et al.*, 1987; Julesz, 1981) and refer to what Bergen calls a "micropattern" which is repeated randomly throughout the texture. Both have abandoned the notion that the spatial arrangement of these micropatterns is discriminatory and refer simply to the numbers or density of the micropatterns, especially as a function of the size of the micro-

sible boundaries around the "true" boundary location. This work has largely been focused on digitizing error (Goodchild, 1989). The problem of estimating the epsilon band width has been dealt with in this latter context, for example, by means of theoretical estimates (Dunn *et al.*, 1990) based on details of the digitizing process. Hence, because digitizing errors are confined to the immediate neighborhood of the original lines on the paper map and are expected to be similar throughout the map, a single global estimate of epsilon band width has been assumed. Moreover, a variety of probability distributions have been proposed to describe differences between the digitized line and the original. Alternatively, a global epsilon width is adopted and the amount of "coincident" lines which fall into this zone is estimated. Chrisman and Lester (1991) adopted such an approach in an agricultural context.

In a context where photointerpretation boundary error is likely to be high, the situation is considerably more complex. The epsilon bands (called "fuzzy widths" in this paper) are likely to differ depending on the location and local context of the boundary within the image. It is not clear that a useful global estimate can be obtained. Second, the errors are much larger than in the case of digitizing errors. In one discussion of the latter, a normal probability distribution function is excluded on the grounds that this permits boundaries to be mislaid very large distances (Dunn *et al.*, 1990). In aerial photointerpretation, such large errors are not infrequent and certainly cannot be excluded. Third, understanding digitizing errors has tended to focus on the boundaries, to the exclusion even of polygons (Dunn *et al.*, 1990). Yet boundary uncertainty is a function of adjacent polygons and cannot be studied or understood in terms of isolated polygons (Pullar, 1991). Hence, while the techniques developed for measuring digitizing error can be used for characterizing photointerpretation boundary uncertainty, adjustment for the many contextual differences must be made.

Human and Computer Vision Research

It is also instructive to examine the scientific literature on computer vision as it relates to texture discrimination. Ber-

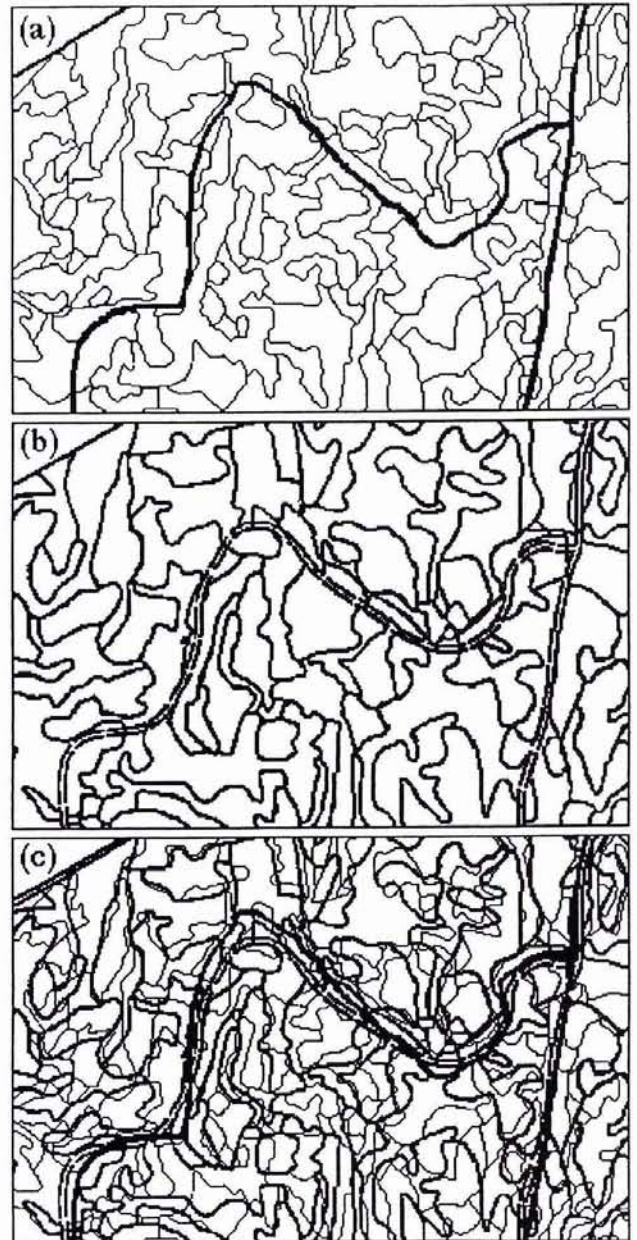


Figure 2. In (a) and (b) are shown two forest maps of the same area, produced from interpretation of aerial photographs at different times. In (c) is shown an overlay of the two maps.

pattern. Caelli (1985, 1986) has developed a three-stage computer algorithm based on this kind of analysis. The first stage consists of what Caelli calls *impletion*, or the process whereby excitation from strongly responding areas spreads to weakly responding areas, thus filling in areas which contain little or no structure. His second stage consists of *correlation*, which looks for agreement between outputs of different frequency filters at a given location (e.g., a "scale-hunting" function), while his third stage consists of *grouping*, which seeks to assign pixels or features to regions in such a way as to maximize the correlation between values within regions and minimize it between regions. In 1986, Caelli introduced an additional level which involves *adaptively seeking descriptors* that yield regions of uniform structure.

This work provides support for the central hypotheses of this paper. Our focus is not on texture segregation as such, but on an attempt to characterize the spatial error which can be associated with texture boundaries as they emerge from human visual processing. Although there has been a great deal of work on texture segmentation and discrimination, very little has focused on spatial uncertainty in boundary placement. Reed and Wechsler (1990) note that texture analysis involves simultaneously maximizing spatial and spatial frequency resolutions – something that cannot be done. Wilson and Granlund (1984) have discussed this same problem as an extension of the Heisenberg uncertainty principle into the area of pattern recognition and signal processing. However, none of this work has attempted to quantify the spatial uncertainty involved in boundary placement.

The work discussed by Bergen (1991) indicates that texture discrimination must be simple. In this paper, which is focused on evaluating the spatial uncertainty of boundary placement, we have adopted as simple a model of texture as possible. Our approach is very similar to that described by Bergen, because we attempt to identify a characteristic micropattern for each texture. This is defined by a region of sufficient size that the micropattern is stable throughout a larger textured region. This micropattern is extracted in terms of a measure of homogeneity. Because we are interested in spatial uncertainty, we have identified several factors as contributing to this uncertainty. First, the size of the micropattern and its relative spacing. Second, the variability within the texture, which contributes to the spatial uncertainty. And third, we label other effects which are more difficult to quantify, "local context effects," because we believe that they are largely related to human visual processing of neighborhoods. Our work is a first study on the characterization of spatial uncertainty in texture segmentation, focused especially on photointerpretation. We hope that the work will be generalizable enough to eventually provide uncertainty estimates for automated texture segmentation as well, or at least that the work will serve as a useful reference for others attempting to do so. This paper is *not* intended to be a "final" or definitive study for boundary uncertainty characterization in texture segmentation, whether it be based on human visual processing or independent computer processing.

General Procedures

The first concern for understanding boundary uncertainty in maps obtained from aerial photointerpretation is to obtain reliable measurements of this uncertainty. However, under most circumstances in forestry, the true boundary location is unknown and hence cannot be used as a reference. Proposed solutions include least-squares polynomial fitting through the digitizing points of the boundary (Gong and Chen, 1992), corridor generation techniques (Aubert *et al.*, 1994), and clustering of boundary curves (Edwards, 1994). Most of these techniques are encumbered by the complexity of the bounda-

ries produced by photointerpretation (Gong and Chen, 1992; Edwards, 1994), so that once each boundary has been isolated, measurement is possible, but isolating the appropriate boundaries is difficult.

We have broken the development of a theory of photointerpretation uncertainty into stages. The first stage is to estimate boundary uncertainty for synthetic textures using an "absolute" ground truth (i.e., the spatial partition used to define the synthetic images). This allows us both to isolate the limitations of photointerpretation in terms of a "real" ground truth and to test some of the basic premises of our approach. For example, we can quantify some of the effects of local neighborhoods on boundary uncertainty. Also, we have stated that we believe that boundary uncertainty (width) is related to the texture patterns on both sides of a boundary, and not on the texture characteristics of a single polygon. This first experiment allows us to test this hypothesis. The use of artificial textures is not a major drawback, because the perceptual processes involved are very similar, if not precisely the same, to those used by interpreters of aerial photography. The second stage is to generalize this work to the case where the ground truth is unknown (preliminary results on this second stage have been reported elsewhere – see, for example, Aubert *et al.* (1994) and Edwards (1994)). And the third stage is to adapt the resulting theory to a real photointerpretation context. In this paper, we shall present the results of the first stage of the study.

There are several challenges which must be overcome in order to be able to use this approach successfully. As mentioned, techniques for evaluating the width of the uncertainty function associated with each boundary, based on the photointerpretation process, must be developed. Techniques for representing these boundary widths and for carrying out overlay operations must also be examined, and spatial data structures which support these approaches may need to be developed if they are to be integrated into GIS. Fuzzy set theory (Zadeh, 1965) provides one framework for addressing the analysis issues using fuzzy uncertainty (e.g., Altman, 1992; Burrough, 1989). However, the single most difficult obstacle to using this theory consists of characterizing the "shape" of the uncertainty relation correctly. This paper presents results related to the development of techniques for evaluating the width and shape of "fuzzy" boundaries. This work has been developed with respect to characterizing uncertainty in the context of forestry, but could be applied to any context with similar kinds of uncertainty (including soils mapping).

Experimental Motivation and Hypotheses

Presently, global, not local, errors are used in GIS and remote sensing to characterize data. For example, in remote sensing a "confusion matrix" is usually determined to characterize classification error. This confusion matrix and derived quantities such as the overall accuracy (Lunetta *et al.*, 1991), the kappa coefficient (Rosenfeld and Fitzpatrick-Lins, 1986), the user's error, and the producer's error (Story and Congalton, 1986) are all *global measures of error*. That is, they are obtained by evaluating and summing across the entire classified image (or that part for which "ground truth" is available). It is not possible to obtain a reliable local error estimate from these values. It is known, for example, that many classification errors are context dependent (Chrisman and Lester, 1991). But global error measures do not allow one to map such context dependencies. Other examples of global errors are digitizing errors in GIS, registration errors in remote sensing, and DTM errors; the usual quoted errors apply uniformly to an entire region (map or image) and do not take into account local variability in these measures.

In addition to quantifying local error, a secondary goal

was to understand better how photointerpretation is done. Does the photointerpreter attempt to identify uniform regions, or does the photointerpreter look for differences or "edges" which are significant enough and representative enough to map? Texture discrimination is known to involve both processes (Bergen, 1991). In Caelli's algorithm (Caelli, 1985), texture edges appear to emerge during the second phase (correlation), which occurs in the spatial frequency domain. Indeed, some measure of local homogeneity seems to emerge at this stage. Grouping into larger homogeneous regions appears to occur at the third stage, based on correlation measurements obtained at the second level. This suggests that photointerpretation proceeds by first generating "local" homogenous regions and boundaries, which are later grouped into larger regions and are classified into categories.

The idea that the photointerpreter follows a local texture difference suggests that the uncertainty in the boundary's placement is related, initially, to the scale of the texture variability on both sides of the boundary, and second, to some measure of difference between the two textures. These assumptions guided the analysis phase of the project, which was devoted first to test for the existence of such relationships, and second, to quantify mathematically their form.

It is also worth noting that multispectral image classification is not a dissimilar process. Texture segmentation techniques (Reed and Wechsler, 1990) result in boundaries which behave similarly to interpretation boundaries. The major difference is that any given segmentation software will generate the same boundary every time it is run. However, different software and different parameters such as thresholds used in such software will produce different boundaries (Goodchild, 1988), and the differences are likely to be linked to similar causes as for photointerpretation. Very little work on boundary uncertainty has been carried out with regard to remote sensing image analysis.

The use of the word "texture" here is intentionally specific. We believe that much of the photointerpretation task is related to finding differences in texture patterns as well as image tone. The experiment design parallels the approaches taken by researchers studying human texture discrimination in that it consists of simulating textures, eliciting responses (in the form of interpretations), and analyzing the results in terms of the simulated textures. For the purposes of this experiment, we constructed fairly simple textured images with no spectral component, no mixtures of different textural components, and no three-dimensional (stereo) component. The images do contain both textural and tonal differences, however, and hence contain the core features to be expected in photointerpretation.

Furthermore, experience with a variety of standard, statistical image textural measurements led us to avoid using such measurements, at least in these early phases of the analysis. Standard texture measurements such as the co-occurrence measures (Haralick *et al.*, 1973) and derivative techniques such as the density of Laplacian edges (Rosenfeld and Thurston, 1971), etc., are difficult to relate to perceived texture differences. The approach to texture characterization we have adopted is much closer to the structural texture analyses discussed by Haralick (1979) than to the widely used statistical methods.

The Data Set and Analysis Techniques

In order to understand the relationships between forest textures and the interpreters' choices of boundary, a set of three artificial images was created (Figure 3). These images were constructed using a set of carefully designed parameters and a random number generator operating within the framework of these parameters. These images look similar enough to black-and-white images of the natural forest taken at rela-

tively detailed scales that the interpreters had no difficulty imagining the task as a real interpretation task.

To construct the images, a polygon mask was created so as to present both well-defined polygons and a variety of special cases we wished to examine, such as thin bottle-necks, small polygons, etc. Each polygon was assigned to one of six classes. Two different masks were created in this way (Figure 4). For a given class, a "grid" of tree-like shapes was generated. Each "tree" consisted of an intensity hemisphere, defined by the following equation:

$$i = I_o' \sqrt{1 - (r/R_o')^2} \quad (1)$$

where i is the local (i.e., pixel) intensity, I_o' is the peak intensity, r is the distance from the center, and R_o' is the radius of the "tree." These hemispheres were designed to simulate forest crowns with nadir viewing and the sun at zenith (i.e., no shadowing). Furthermore, for a given class, the peak intensity and tree radii are constructed from a class mean and random deviate with a class-specific variance: i.e.,

$$I_o' = I_o + k\sigma_i \quad (2)$$

and

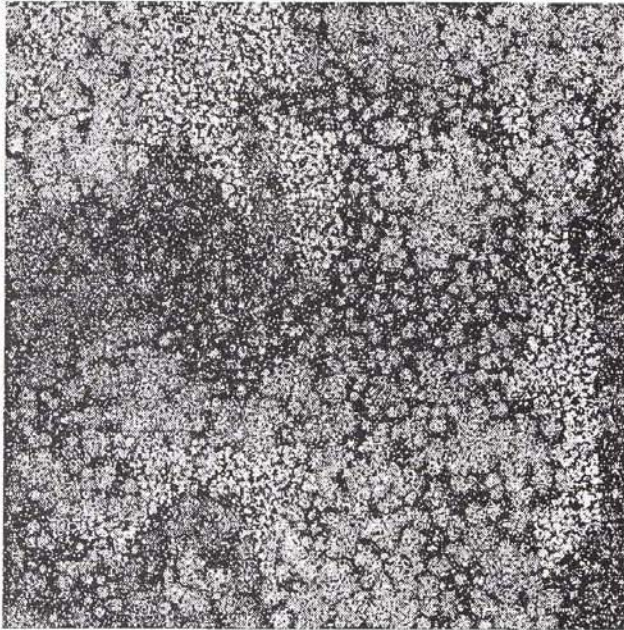
$$R_o' = R_o + l\sigma_R \quad (3)$$

where I_o is the mean peak intensity for the class, R_o is the mean tree radius for the class, σ_i is the standard deviation of the intensity for the class, σ_R is the standard deviation of the radius for the class, and k and l are random deviates following a normal distribution centered on zero with variance 1. The separation parameter was handled in a slightly different manner than the other two. The class-specific standard deviation of the separation parameter was used to define a normal distribution about the grid point specified by the mean separation for that class: i.e.,

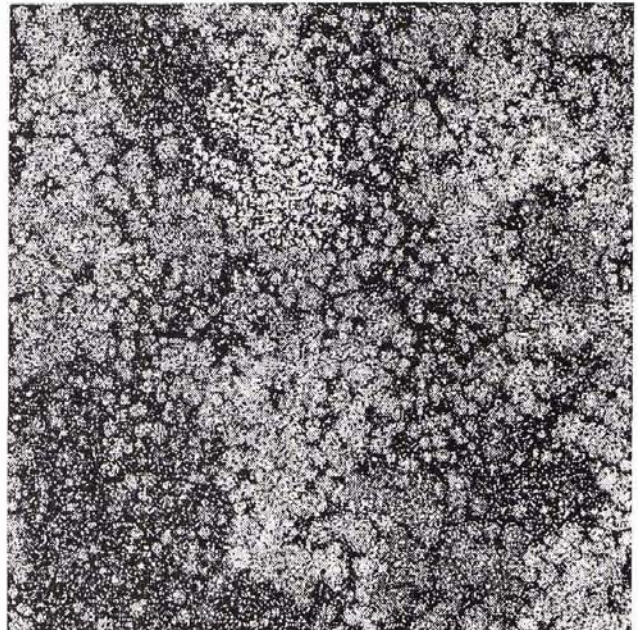
$$\begin{aligned} x &= n \delta x + p \sigma_D \\ y &= m \delta x + q \sigma_D \end{aligned} \quad (4)$$

where x and y are the coordinates of the tree, δx is the mean separation, n and m are integers which specify the grid coordinates of the tree placement, σ_D is the class-specific standard deviation for the tree displacement off the grid point, and p and q are random deviates following a normal distribution centered on zero of unit variance. The process of constructing a texture for each class then consists in defining values for each of these six parameters (i.e., I_o , σ_i , R_o , σ_R , δx , σ_D) and of using a random number generator to derive the appropriate normal distributions for each of the three variables (intensity, radius, and separation). All values of i and r less than zero were reset to zero, disturbing slightly the strict normality of some of the data sets. Two sets of six parameters were created in this way (Table 1 and Table 2). Both sets of parameters were used with Mask #1, the first set for Image #1 and the second for Image #3. The first set of parameters was also used with Mask #2 to create Image #2. The parameters have been fine-tuned somewhat to generate more realistic-looking forest textures at an apparent scale of about 1:5000. The final stage of image construction consisted in adding a constant background to all images (40 intensity levels) and adding a random Gaussian noise (four intensity levels). The latter leads to images with a level of pixel-to-pixel variation similar to that encountered in real images of the forest and ensures that interpreter attention is not focused on individual "tree crowns" but, rather, on the texture patterns.

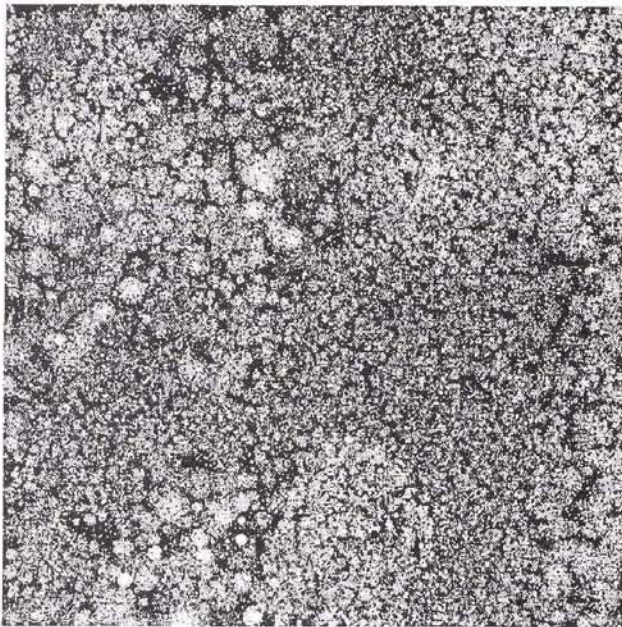
The use of a grid for assigning the placement of the "trees" may seem questionable. However, of importance for this study was to be able to parameterize the distribution, and to ensure that the generated textures were of sufficiently random appearance that the perceptual processes involved



(a)



(b)



(c)

Figure 3. The artificially generated images used in the photointerpretation studies. (a) Image #1, produced by Mask #1 using texture Category Set #1. (b) Image #2, produced by Mask #2 using Category Set #1. (c) Image #3, produced by Mask #1 using Category Set #2.

would be similar to those engaged in real interpretation. Studies such as those described by Bergen (1991) support this approach, because the spatial arrangement of texture elements has been shown to be less important in perception than is the density of the elements. Furthermore, from a forestry perspective, a grid with random deviations is no better and no worse than a purely stochastic placing of crowns, and both have been used in a large number of computer simulations for varying purposes.

All three images were interpreted by the same nine people. These were mostly students, some with previous photointerpretation experience, some without. Each interpreter was told that there were "between three and ten classes present in each image," in order to restrict the range of distinct

categories which might be found. In conventional photointerpretation, interpreters work with libraries of known texture patterns and hence also with a limited number of categories. Our interpreters were also told to apply a minimal mapping unit of one square centimetre to the interpretation (i.e., to group polygons smaller than this with adjacent polygons). This is also similar to the conventional interpretation procedure, in which a minimum mapping unit is employed. The order in which each subject interpreted the images was randomized. Some examples of the interpretations for Image #1 are shown in Figure 5.

Because analysis techniques were based on a variety of concepts, greater detail is provided. The goal of this work was to characterize the fuzziness of the boundaries between

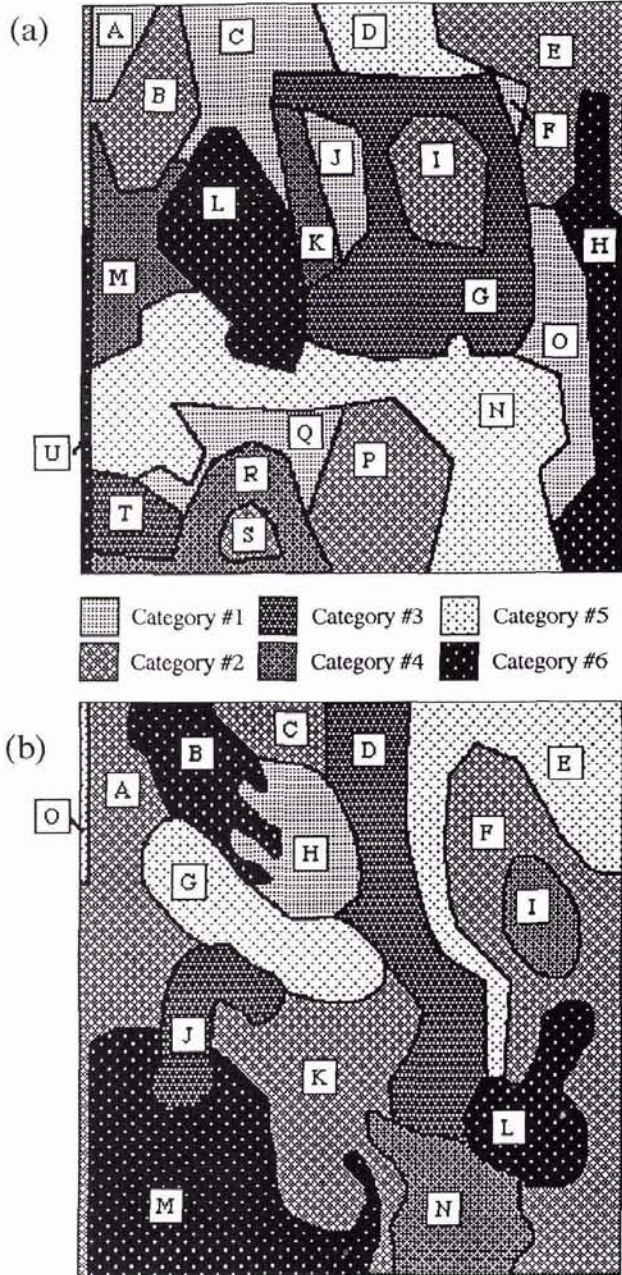


Figure 4. The two masks used to generate the images shown in Figure 3. (a) Mask #1. (b) Mask #2. Shown also are the polygons labels.

may be possible to characterize boundary uncertainty as a profile along the boundary, we have limited our attention to an average boundary uncertainty width for a boundary segment of a given twain. It is further hypothesized that the width of the fuzzy boundary (i.e., a measure of the interpreter-to-interpreter difference in the boundary location) is inversely related to the difference in texture between the two polygons on either side of the boundary. The larger the perceived difference in texture patterns, the smaller the difference will be between interpreters when defining the boundary, and vice versa. When the difference in texture patterns is perceived to be very small, the boundary may not be detected at all. Thus, a second contribution to the fuzzy width must be some measure of variability of the texture on each side of the line.

The focus on the twain imposes three additional conditions on the analysis, considered to be a kind of "local context." The first consists of the necessity of having a twain of sufficient length to distinguish the two polygons on either side. If the boundary is too short compared to the size of the texture grain on one side or the other, then few interpreters will be able to find the boundary (polygons C and M in Mask #1, Figure 4a). The second condition is that if the fuzzy width is larger than the polygon width, then the polygon will be severely fragmented or even will cease to exist. Therefore, fuzzy widths larger than this value will not be seen. This introduces a bias against very large boundary uncertainties in the analysis. Hence, the boundaries obtained from each interpretation must be validated against the mask and cases of absent boundaries must be identified.

A way of identifying these contextual effects has been developed and implemented. The approach depends, however, on the ability to measure a spatial uncertainty value characteristic of the variability of each texture. The value used is the square root of the minimum surface area needed to characterize the texture pattern's variability, derived directly from the parameters used to generate the texture patterns. The details of this formulation are given in the next section. This distance measures the "fuzziness" of the edge of a textured region in isolation from other textured regions. It is a local measure consistent with recent work on texture discrimination (Reed and Wechsler, 1990). For each polygon in the mask of a given image, and for its appropriate texture parameters, the characteristic scale of variability of the texture is determined. The interior corridor or buffer zone limit of the polygon determined using the characteristic variability scale is computed (Figure 6a): i.e., a different corridor width

TABLE 1. CATEGORY SET #1

Category	I_0	σ_t	R_0	σ_R	δx	σ_D
1	45	7	1	1	2	2
2	40	4	4	3	6	3
3	35	3	4	1	9	4
4	25	4	7	3	12	3
5	35	3	5	3	9	3
6	25	6	2	2	8	3

TABLE 2. CATEGORY SET #2

Category	I_0	σ_t	R_0	σ_R	δx	σ_D
1	35	6	5	3	9	3
2	40	10	2	2	3	3
3	35	5	4	1	5	3
4	40	20	7	3	9	3
5	30	5	3	1	4	2
6	40	8	4	3	6	3

polygons. This idea itself is based on the assumption that there may not be a hard and sharp line separating one forest stand from another (there usually isn't!). Because of this, boundaries between stands are not expected to be razor sharp as depicted on conventional forest maps. The standard means for evaluating the precision of forest maps (or any cartographic theme) are global, area-based approaches. This includes the use of confusion matrices in remote sensing or comparison of random sample plots with map polygons. We would like to have a local, boundary-based approach.

The basic tenet underlying the analysis techniques is that the smallest unit of interest is a polygon pair and its common boundary (we call this unit a "twain"). Although it

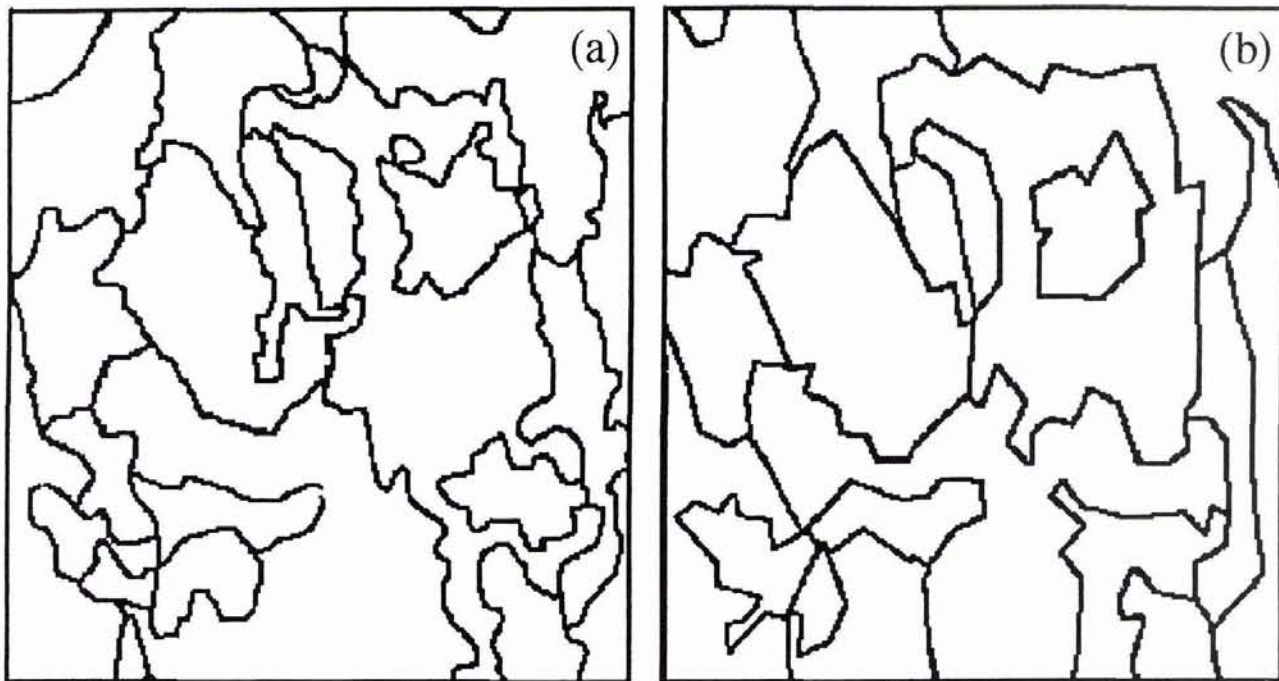


Figure 5. Two interpretations of Image #1.

is applied to each polygon boundary in the mask. This leaves a map of polygon "nuclei" with corridors between each nucleus. Any polygons which were too small to properly characterize the texture will have been removed at this stage. A new corridor (called the "outer polygon boundary") is then generated around each nucleus, using the same corridor width as earlier (Figure 6b). Note that these corridor operations are equivalent to a morphological opening and closing of the polygons (Serra, 1982).

The inner polygon boundary can be considered to enclose the region within which the texture can be unambiguously perceived and, hence, the region in which the polygon's existence is "stable" (these polygon cores are shaded by category in Figure 6). The outer polygon boundary can be interpreted as the limit of the zone where the polygon's identification has a maximum likelihood of being valid (i.e., maximum likelihood with respect to other polygons). This "variability map" is, from one point of view, a better representation of "ground truth" from the photointerpretation process than the original mask, because it represents the perceivable textured regions for the photointerpretation process. All non-perceivable spatial features have been removed from the original mask. This is not unlike the convolution of an ideal signal with an instrument response function as is practiced in signal processing (see Tobler, 1969), resulting in an appropriately degraded ground truth map. In Figure 6c, the nine interpretations acquired for Image #1 and shown in Figure 1 are superimposed on this polygon-specific variability map. It can be seen that the boundaries in this mask correspond closely to the observed interpretation boundaries. There are some areas where polygons are more fragmented in the interpretations than in the original, but the contrary rarely occurs. The exception appears to be Category #6, which has a high variability scale (see next section) but a low mean intensity. As explained in the next section, these regions contribute little to boundary error because of their low mean intensity.

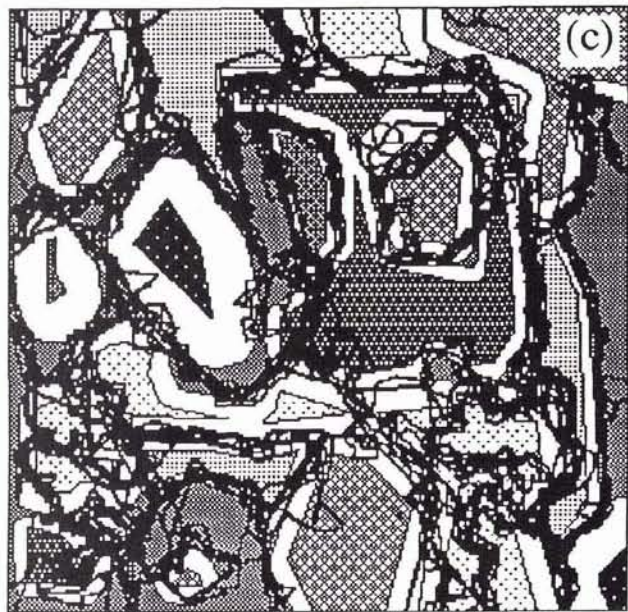
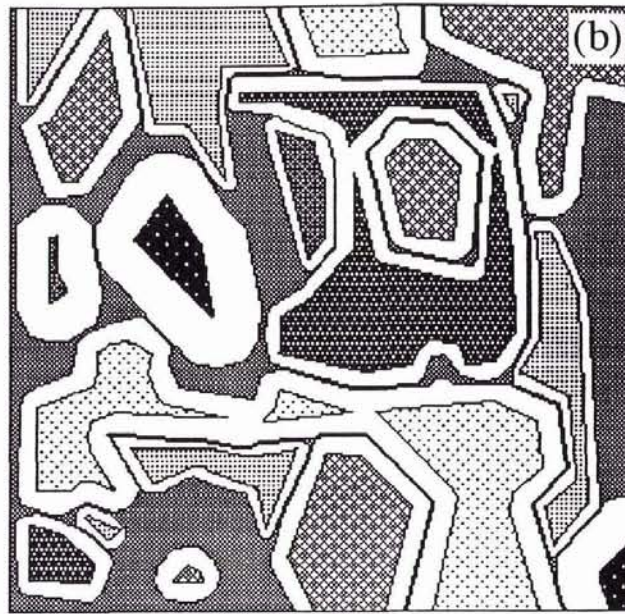
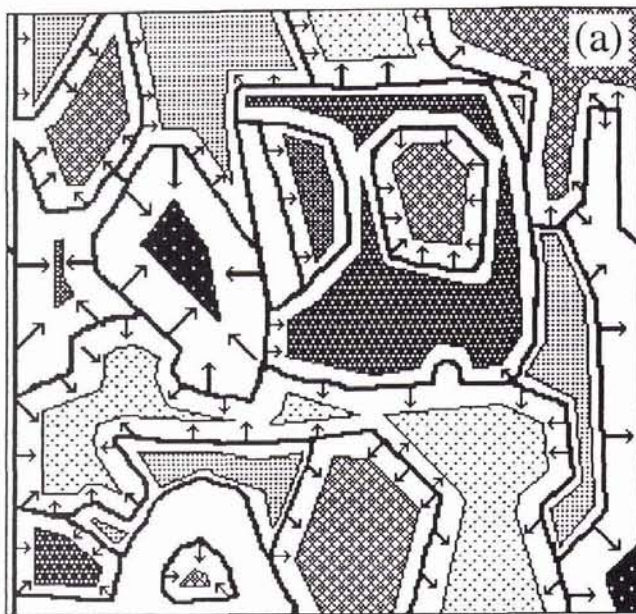
This method of determining a polygon-specific variabil-

ity map in terms of stable nuclei and unstable boundaries is central to the analysis presented in this paper. It does not address, however, the problem of inclusions of "minimum mapping units" as used in photointerpretation practice. This latter consists of small regions which have been grouped into the larger regions because they are too small to map individually. We have chosen to focus on boundary uncertainty directly, by comparing interpreted boundaries against a "degraded ground truth" computed as described above. The problem of inclusions becomes more important when there is no independent ground truth available.

Note that the new outer boundaries correspond to the old polygon boundaries in many cases. If we think of the polygons as islands, then there are gaps or "holes" in the new map where the polygons were too thin to adequately represent the texture variability. That is to say, they were too small to be perceived. This new map provides a convenient tool for determining where local context (the proximity effects of nearby spatial arrangements of polygons on the photointerpretation process) disturbs the boundary identification process. Boundary segments for which the new outer boundary matches the old polygon boundary are indicators that the edge between two textured regions is relatively unaffected by local context, whereas old boundary segments which are affected by local context have now disappeared. Using this map (Figure 6b), we can remove all cases where an old boundary segment has disappeared from the analysis.

For the boundaries which have remained unchanged after the corridor operations, we can reasonably expect their associated boundary measurement errors to be related to the difference in texture pattern on both sides. Hence, we can average derived widths from several twains. The procedure is complicated by the fact that different interpreters will tend to discriminate less well and will fail to see some small regions which others have no difficulty finding. These differences among interpreters need to be removed from the sample before analysis proceeds.

The boundary uncertainties (or "measured fuzzy







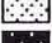




-  Category #1
-  Category #2
-  Category #3
-  Category #4
-  Category #5
-  Category #6
-  Corridors
-  Holes
-  Set of interpretations

Figure 6. The process of producing a variability map from the image mask (for Image #1). (a) Beginning with the mask, generate polygon-specific corridors based on the texture variability alone. This results in the identification of "core" polygons which can be found by an interpreter. (b) Generate the inverse corridors from the core polygons. This leaves holes where polygon identification is confused. In (c), the resulting map is compared to the nine superimposed interpretations from Image #1 (see Figure 1).

widths") for the nine interpretations were determined by generating a "proximity map" in a raster representation for each of the interpretations. This proximity map converts every pixel to a measure of its distance from the nearest boundary. Then the average "proximity measure" for the locations of each boundary on the mask, with respect to the interpreter proximity map, was determined. Furthermore, the proximity measures were assigned a positive or a negative value depending on which side of the line they fell. This allows one to define a random error, utilizing the sum of the

absolute values of the displacement errors, and a systematic error, utilizing the sum of the relative values of the displacement errors. The systematic error measures displacements which are systematically towards or away from a given texture class. The random error was considered to be the desired measure of "fuzzy width." Note that the approach adopted produces an approximation of the fuzzy width which is a little different from standard error analysis procedure, which would consist of a root-mean-square estimate (for a more rigorous approach, see Aubert *et al.* (1994)). Be-

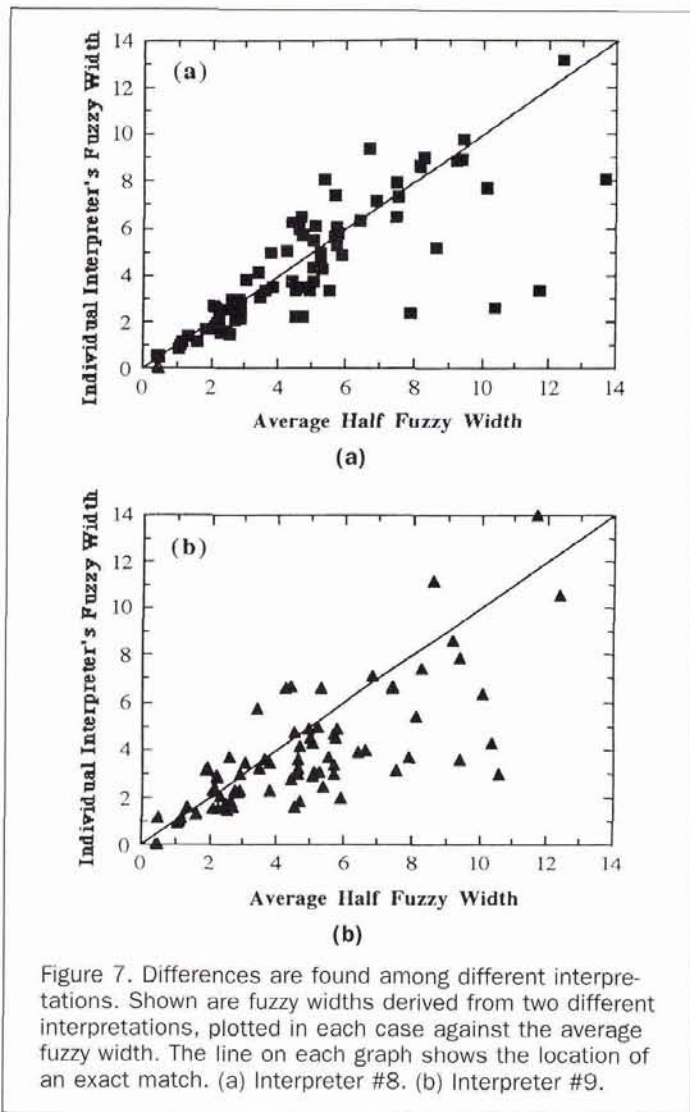


Figure 7. Differences are found among different interpretations. Shown are fuzzy widths derived from two different interpretations, plotted in each case against the average fuzzy width. The line on each graph shows the location of an exact match. (a) Interpreter #8. (b) Interpreter #9.

cause the purpose of this study was to test the existence of a relationship between boundary uncertainty and characteristics of the texture pair, an approximation of this kind was deemed adequate. Following this, all nine fuzzy widths were averaged together to produce a mean measure for each twain.

By plotting the fuzzy widths of an individual interpreter against the mean fuzzy width for each twain, one can see the effect of interpreter bias (Figure 7). In fact, there appear to be two parameters of importance. Some interpreters obtain systematically lower fuzzy widths than do others. Also, some interpreters are more consistent, whereas the fuzzy widths for others vary wildly about the mean. Although there does not appear to be any systematic trend with previous photointerpretation experience, no general conclusions with regard to photointerpretation practice can be drawn because these images are not standard aerial photographs.

Once the mean fuzzy width has been estimated, the twains which are likely to be affected by local context are removed from the sample. The analysis then consisted of attempting to obtain a relationship between the parameters used to generate the image textures which characterize the texture discrimination, and the measured mean fuzzy widths for each pair of categories which are spatially contiguous on the map. That is, we average fuzzy boundary width over all

boundaries between pairs of polygons with similar categories and relate them to the image texture parameters.

Results of the Analysis

Global Classification Error

We begin the analysis with a more standard way of estimating error: the use of a global classification error such as discussed earlier on. This is done in order to provide a baseline analysis for comparison with other studies, to provide some insight into category classification errors, and, also, to highlight some of the advantages of the local error analysis proposed in the paper compared with more traditional global approaches.

A single confusion matrix was developed for each image (Tables 3 to 5) by averaging over all nine interpretations. For each cell in the "mean" confusion matrix, the mean number of pixels over all nine interpretations was tabulated. In the case of interpreters who found more than the six classes as defined by the masks, all additional classes were grouped together and tabulated under "Other" (such a practice did not significantly affect the results – about 4 percent of pixels were classed into the category "Other"). A modified kappa coefficient (κ) was also calculated for each image (Foody, 1992). The kappa coefficient accounts for errors of omission and commission, whereas the standard classification accuracy measure does not.

Global accuracy (i.e., the agreement between the interpreted images and the mask used to generate the images) ranged from 53 percent for Image #3 to 67 percent for Image #1. Similarly, κ ranged from 0.454 to 0.541. While κ is large enough to suggest that the classifications are not completely random ($\kappa = 0$), the global accuracy demonstrates that different interpretations of the same images have a remarkable amount of dissimilarity. Certainly in the case of Image #3, almost half the image is "incorrect" or "uncertain." It is argued here that this reinforces the approach of examining local error in general, and boundary error in particular, because *a priori* much of the global error may be spatial-context specific. For example, Chrisman (1982) found that as much as 18 percent of surface area was contained in even small epsilon bands around map boundaries. Furthermore, the evidence seems to indicate that the accuracy of "real" photointerpretation is not much better than for our artificial images (Biging *et al.*, 1992).

Furthermore, comparing the classification accuracy per category between Table 3 (Image #1) and Table 4 (Image #2) shows some startling differences between the two images, even though the textures are the same. For example, the interpreters identified correctly 40 percent of Category #5 in Image #1 but only 13 percent in Image #2. The differences for many of the other categories are equally striking. The most variable results are clearly those for Categories #2 and #5, the most variable textures. These results indicate that local context may play a much larger role in interpretation accuracy than heretofore believed.

The off-diagonal elements of Tables 3, 4, and 5 also suggest that global error estimates are an inappropriate quantification of uncertainty for many mapping purposes. On Images #1 and #2 – generated using the same image parameters but different masks – it is evident that Categories #2 and #5 were highly confused. However, at locations where a boundary between polygons of Types #2 and #5 was identifiable, the fuzzy widths of the boundaries were relatively small (see next section). Thus, the local context of each boundary (its length, the size of the polygons on either side, etc.) is important to both the global and local error.

This is not to suggest that only boundary error is impor-

TABLE 3. EVALUATION OF GLOBAL IMAGE CLASSIFICATION (IMAGE 1). (VALUES IN EACH CELL ARE THE MEAN NUMBER OF PIXELS OVER ALL NINE INTERPRETERS.)

		Truth (Mask)						
Category		1	2	3	4	5	6	Total
Interpretation	1	19203	914	842	484	497	1195	23135
	2	2924	20165	1431	873	9123	975	35491
	3	1575	2917	18339	1258	6915	255	31259
	4	778	807	335	10351	679	668	13618
	5	1131	8360	682	1504	13427	596	25700
	6	415	354	2994	1904	2567	15554	23788
Other		309	1953	435	306	423	3583	7009
Totals		26335	35470	25058	16680	33631	22826	160000
% Correct		73	57	73	62	40	68	61

$$k = (0.6065 - 0.1674)/(1 - 0.1674) = 0.5274$$

$$k' = (0.6065 - 1/7)/(1 - 1/7) = 0.5409$$

(Kappa has been calculated by adding an additional column to Table 1 for "Other" to make it symmetrical. This column sums to zero.)

TABLE 4. EVALUATION OF GLOBAL IMAGE CLASSIFICATION (IMAGE 2). (VALUES IN EACH CELL ARE THE MEAN NUMBER OF PIXELS OVER ALL NINE INTERPRETERS.)

		Truth (Mask)						
Category		1	2	3	4	5	6	Total
Interpretation	1	5928	487	439	0	44	248	7146
	2	574	44700	2045	1192	15420	3605	67536
	3	85	745	12365	22	3466	1659	18342
	4	0	1174	257	10049	113	221	11814
	5	2	3374	57	240	3408	185	7266
	6	495	2003	6075	289	1986	30427	41275
Other		101	2510	733	713	1779	785	6621
Totals		7185	54993	21971	12505	26216	37130	160000
% Correct		83	81	56	80	13	82	67

$$k = (0.6670 - 0.2355)/(1 - 0.2355) = 0.5644$$

$$k' = (0.6670 - 1/7)/(1 - 1/7) = 0.6115$$

(Kappa has been calculated by adding an additional column to Table 2 for "Other" to make it symmetrical. This column sums to zero.)

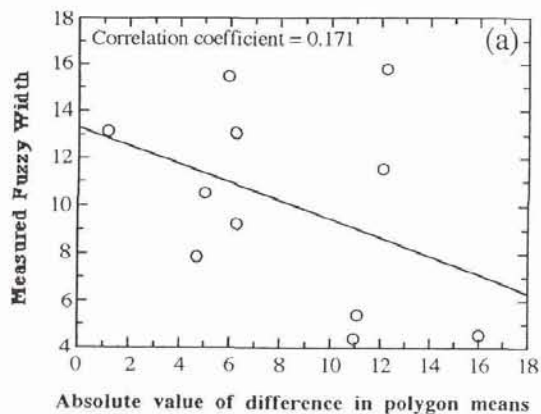
TABLE 5. EVALUATION OF GLOBAL IMAGE CLASSIFICATION (IMAGE 3). (VALUES IN EACH CELL ARE THE MEAN NUMBER OF PIXELS OVER ALL NINE INTERPRETERS.)

		Truth (Mask)						
Category		1	2	3	4	5	6	Total
Interpretation	1	9866	895	2145	3452	1220	2947	20525
	2	925	21538	866	139	711	3161	27340
	3	3645	2256	11539	979	3426	3005	24850
	4	2881	4013	356	10246	835	6143	24474
	5	5756	1220	9464	1590	26822	1140	45992
	6	2461	532	481	84	343	5243	9144
Other		801	5016	207	190	274	1187	7675
Totals		26335	35470	25058	16680	33631	22826	160000
% Correct		37	61	46	61	80	23	53

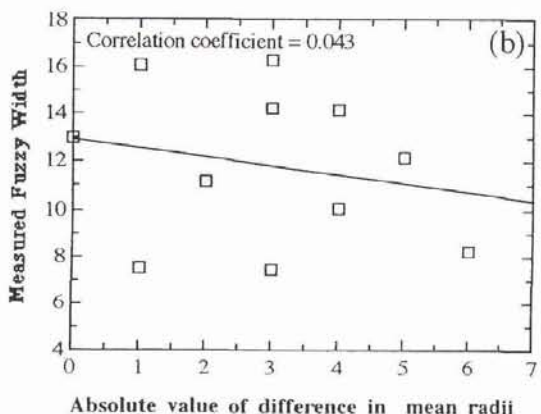
$$k = (0.5328 - 0.1678)/(1 - 0.1678) = 0.4386$$

$$k' = (0.5328 - 1/7)/(1 - 1/7) = 0.4549$$

(Kappa has been calculated by adding an additional column to Table 3 for "Other" to make it symmetrical. This column sums to zero.)



(a)



(b)

Figure 8. (a) Half fuzzy width versus difference in mean polygon intensity. (b) Half fuzzy width versus difference in mean radius.

tant. Chrisman and Lester (1991) have noted that both boundary and category error should be considered in error models. While this paper is concerned with the quantification of boundary error, it is recognized that regions of similar texture occupy the interiors of the boundaries, and that boundaries are an expression of the perceived existence of two regions of different texture. In cases where two texture patterns are similar in appearance and hence highly confused, many additional and spurious boundaries may be identified by the interpreter, and the resulting confusion in the classification of these regions will increase the off-diagonal elements for these categories. The analysis developed in the following section does not explicitly deal with such cases and is, therefore, not all-inclusive. However, the strength of the fuzzy-width boundary models developed in this paper suggests that this approach can lead to significant gains in understanding of local error and hence improve map-to-map compatibility (see also Aubert *et al.* (1994) and Edwards (1994)).

Local Boundary Error

In the second part of the analysis, the relationships between the measured fuzzy widths and simple combinations of the texture parameters were examined. Figure 8 shows the absolute value of the difference in mean intensity between the two polygons of each twain plotted against the measured fuzzy width. There is no apparent relationship between the two (r^2 less than 0.1 for both diagrams).

Following this, an attempt was made to identify the factors which contribute to the visual discrimination process. Given the assumption that the two classes of factors which contribute are the texture variability and the texture differences, this analysis led to a number of new observations. The variability of the texture was clearly not well characterized by the variance around the mean intensity. Rather, the variability was recast as the minimum region size which characterizes the full range of the texture pattern. The larger this region size, the higher the "variability scale" of the texture. This idea of variability scale was measured, in terms of the image parameters, by defining a threshold value of three standard deviations, and determining the minimum number of objects ("trees") required to "fill out" the Gaussian distributions in intensity, separation, and radius to this threshold. Note that this is not a measure directly related to individual pixels. The minimum number of objects (N) needed for any one of these distributions is given by the requirement that the error around the known mean be inferior to a threshold value: i.e.,

$$\sigma_{\text{thres}} = \frac{\sigma}{\sqrt{N}} \quad (5)$$

which, when rewritten, gives

$$N = \left(\frac{\sigma}{\sigma_{\text{thres}}} \right)^2 \quad (6)$$

After some experimentation, a σ_{thres} threshold of 10 percent of the mean peak intensity and 20 percent of the mean radius was adopted. The two numbers are then multiplied together to obtain the number of individual "trees" needed to characterize the pattern (because the two distributions are constructed independently). Following this, the mean area occupied by each object (i.e., the square of the mean separation between objects) provides the additional scaling factor allowing the texture pattern's "characteristic area" to be determined: i.e.,

$$A = \left[\frac{\sigma_I}{0.1 I_o} \frac{\sigma_R}{0.2 R_o} \right]^2 (\delta x)^2 \quad (7)$$

The square root of this characteristic area is, hence, a measure of the expected displacement uncertainty related to the variability of the texture pattern. However, there is an added complication. In order to determine the contribution to the fuzzy width of this parameter, the variability of both textures of the twain must be combined in some way. Simply adding the two variabilities explained some of the fuzzy widths but left others completely out of the expected range.

Careful visual inspection suggested that the variability of a very bright texture dominates the boundary displacement error if the second texture is faint, no matter how variable the latter. By weighting the square root of the characteristic area by the mean peak intensity of the texture,

$$V = \frac{\mu_i \sqrt{A_i} + \mu_j \sqrt{A_j}}{\mu_i + \mu_j} \quad (8)$$

where V is the variability measure for the boundary, i and j are the different categories of the twain, and μ_i and μ_j are the mean intensities for each category, a relatively strong relationship with measured fuzzy width was obtained. This approach is similar to Caelli's first phase of texture segmentation, where regions containing structure are given preference over regions containing little structure (Caelli, 1985).

The third aspect of the analysis consisted of properly characterizing the functional relationship between texture

difference and boundary uncertainty. Which texture differences contribute to the uncertainty? Again, although a correlation between the difference in mean peak intensity and fuzzy width, or between the difference in mean radius and fuzzy width, can be obtained, the dispersion is high. Adding the derived relationships only worsens the fit.

The solution here is to determine the predicted uncertainty for each feature difference independently and then select the smallest. The philosophy behind this is intuitively reasonable. When discriminating between two textures, if the intensity difference is large, even if there is only a moderate difference in radii, the intensity difference is likely to dominate our perception. The difference in radii does not contribute significantly to our ability to discriminate. Such multi-channel effects have been noted before (Julesz *et al.*, 1973) and, indeed, there is some evidence that human visual processing may be based on such procedures (Bergen, 1991).

The analysis consisted, therefore, of adjusting a set of scaling parameters for each feature difference (plus the variability) between the two textures so as to minimize the least squared error of the linear fit to the relationship between variability, feature difference, and measured fuzzy width (Figure 10): i.e.

$$W = \min \left(\frac{g_I}{\delta I}, \frac{g_R}{\delta R}, \frac{g_{\sigma_I}}{\delta \sigma_I}, \frac{g_{\sigma_R}}{\delta \sigma_R}, \frac{g_D}{\delta X}, \frac{g_{\sigma_D}}{\sigma_D} \right) + g_V V \quad (9)$$

where the δ indicates the absolute value of the difference between the feature values on each side of the boundary. It was found that the only feature differences which contribute significantly to the texture discrimination were the difference in mean peak intensity and the difference in mean radius. The differences in the standard deviations, and in the spacing, were also examined but were found not to contribute to the fuzzy width of any of the boundaries. Hence, the final model used to predict the fuzzy width was the following:

$$W = \min \left(\frac{g_I}{\delta I}, \frac{g_R}{\delta R} \right) + g_V V \quad (10)$$

The values adopted for the scaling factors were $g_I = 20$, $g_R = 4$, and $g_V = 0.2$, based on the analysis of Image #1 alone. These values were later multiplied by an additional scaling factor of 1.16 in order to give a better prediction when Image #2 was included in the analysis. From Figure 9, it can be seen that the model succeeds very well at characterizing the measured fuzzy widths of the boundaries. The r^2 for Image #1 alone is 0.95, although this degrades considerably when Image #2 is considered in the analysis (0.6). In Figure 10, the values for Image #3 are included (as crosses), as well as the context affected values from the first two images. It is worth noting that, although the model was developed for Image #1, it was not significantly modified when applied to the other two images, aside from the global scaling factor discussed above. The model has been shown to work, therefore, for more than one set of textures and more than one spatial configuration of textures.

It should also be noted that an additional context effect was discovered when analyzing Image #2. Mask #2 contains many more simple, straight boundaries between polygons than does Mask #1. It was observed that even highly variable textures could be discriminated with small errors when the boundary was a simple, straight edge. This may be related to the human eye's ability to pick out faint linear features in noisy data, or to extend linear sequences of data (Wertheimer, 1958). In almost all such cases, the measured fuzzy width was systematically smaller than the value predicted based on texture discrimination and texture variability. Note also that most of the textures are highly variable and hence

are strongly affected by local context. We have not identified all contextual influences, and context may become even more important when the analysis is adapted to real aerial photos, where individual interpreter expertise is likely to be more important.

There is no pretense that this is the best model for boundary uncertainty estimation, but, rather, one that is demonstrably valid and relatively simple. It should be noted that, aside from the local context effects which were removed from the analysis, the overall boundary errors were relatively low (Figure 7). Even so, boundary error contributes about 10 percent to 15 percent to the classification errors found in the first stage of the analysis. The so-called "local context effects," which were removed from the analysis, also contribute errors of this order of magnitude to the total classification error. The remainder of the error is therefore due to attribute classification error. The analysis techniques developed and presented here allow one to determine some measure of compatibility. Hence, the "fuzzy map" shown in Figure 6b (based on the texture variability estimates), once modified to account for the addition of discrimination error,

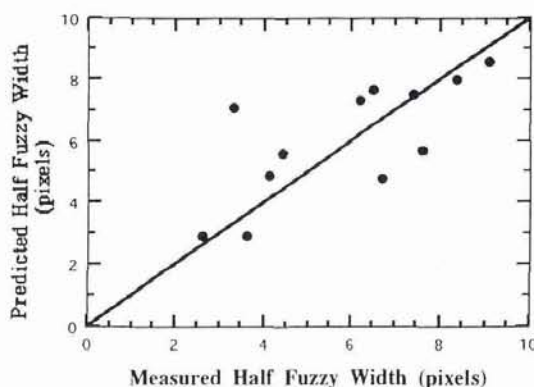


Figure 9. Predicted half fuzzy width versus measured half fuzzy width, based on the use of Equation 10 applied to the category pairs of Images #1 and #2, after category pairs affected by local context have been removed from the sample.

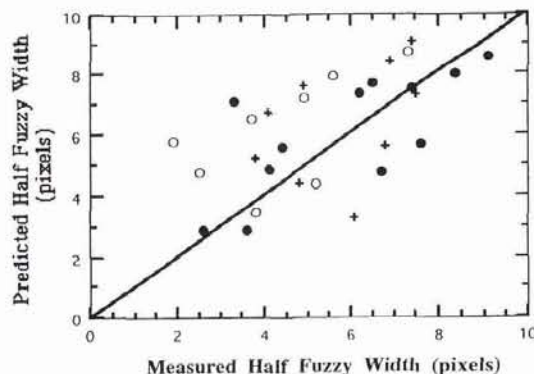


Figure 10. Predicted half fuzzy width versus measured half fuzzy width, for all images and category pairs. The solid circles are as in Figure 9, the empty circles are the context affected category pairs from Images #1 and #2, while the crosses are category pairs from Image #3.

may be used to determine the consistency of a new interpretation of the same image. Procedures for carrying out this kind of analysis have been developed elsewhere (Aubert *et al.*, 1994; Edwards, 1994).

Discussion and Conclusions

The experiment described has allowed us to develop a model which predicts the relative uncertainty associated with photointerpreted boundary placement for a textured image containing forest-like differences in texture. The success of the model indicates that the underlying hypothesis, that boundary uncertainty is related primarily to the properties of the texture patterns on either side and not to the properties of a single polygon, is valid. We introduced the term "twain" to describe a pair of polygons and their common boundary segment, which we adopt as our most local unit of analysis.

It was also found that much of the effect of local context on boundary error can be characterized by looking at texture variability within a given polygon, in isolation from the remaining polygons. Indeed, each polygon can be represented as a central core or nucleus which is relatively stable, and an outer boundary which delimits the region of maximum likelihood. Polygon validity in the "holes" between these outer boundaries must be considered questionable – these are in fact the regions of the map where the effects of local context appear to play a dominant role. In some sense, this map is a more valid "ground truth" than the actual ground truth, because it consists of the perceivable textured regions. In a more complete treatment, this map would need to be further modulated in order to account for texture discrimination. This would allow for correct treatment of Category #6. It is also noted that this approach does not explicitly address the question of inclusions or of different levels of aggregation in the discrimination of textures. However, these are likely to affect polygon interiors just as much as they affect boundaries, and hence may be considered to be a separate (although related) problem.

Additional local context effects were also found. Simple straight edges appear to be easier to discriminate than more complex boundaries and affect the interpreter boundary error. Other effects were noticed but were not explicitly included in the study. These include a wider local context where the presence of a similar texture in the neighborhood may affect an interpreter's ability to "see" a given texture. Over half the boundaries studied were affected by local context effects of some sort, indicating that these effects are extremely important. More work needs to be done to characterize the effects of local context on boundary interpretability.

The specific details of the boundary error model were not intuitively obvious, but do appear to be intuitively reasonable after the fact. The model combines two components, one dealing with texture variability and the other dealing with feature differences between two polygons. The variability term sums two measures of "total pattern uniformity," one for each polygon of the twain, weighted by the mean intensity of each polygon's texture pattern. The feature difference component consists, in this simple model, of the maximum feature discriminator taken from the set of possible discriminators, scaled appropriately so as to minimize the least squares error of the fuzzy width predictor. The model was successful on three different images (with two sets of textures and two spatial arrangements). The model adopted bears some similarity to the perceptual grouping principles proposed by the Gestalt school of psychologists (Wertheimer, 1958), which have been reappropriated within texture segmentation work in recent years (Reed and Wechsler, 1990), and hence at least parallels existing work in human and computer vision fields.

The measures used to characterize both the texture vari-

ability and the texture discrimination could be estimated directly from remotely sensed images. These measures characterize the textures locally and they do so in terms of structural features, a repeatable "texture element" and a statistical pattern of such elements. It could be argued that tools such as the semi-variogram or autocorrelation measures could have been used to characterize the textures. These latter are global statistics, however, while the goal of this work was to develop locally valid analysis techniques.

These findings are significant for a number of applications. They suggest that one can infer at least relative displacement error (and possibly absolute errors, given suitable calibration) based on image characteristics during the photointerpretation process. Furthermore, it may be possible to obtain parameters for interpreter bias which will help compare maps produced by different interpreters (or by the same interpreter at different epochs). Finally, a relatively straightforward method has been found and tested to evaluate and map the presence of some of the local context effects which may affect the photointerpretation process. Although the full benefits resulting from this work must await completion of the second and third phases, the approach appears to be useful. The texture characteristics used in this study, including the "characteristic area," the mean peak intensity, the mean radius, the mean spacing, the variance of the peak intensity, the variance of the radius, and the variance of the spacing are all capable of being estimated from a real image and hence are suggestive of other ways of analyzing texture in the context of forestry, especially for use with very high resolution airborne digital data.

Further work must concentrate on three areas. First, this analysis was carried out using image templates or masks of known characteristics, both spatial and in terms of "attributes." In the real forest, there is no such "ground truth." Hence, these results must be generalized in two ways: first, the photointerpretations must be examined with respect to each other only, rather than with respect to the mask. Second, the textures must be characterized in terms of estimates derived from the image using appropriate image analysis techniques. In order to generalize the work in this way, the problem of pattern scale and hierarchy or inclusions must also be addressed. Indeed, different interpreters worked at different levels of detail in the artificial images studied here. Furthermore, the problem of the effect of local context on boundary uncertainty must be studied in more detail. This problem is linked to the problem of scale.

The second area where more work must be done is to transfer the model developed here to the case of real forest data. Although the details will likely be quite different, the overall approach should be similar. For example, the characteristic areas were weighted by the mean intensity in our model. In the case of an aerial color photo, the relevant weighting parameter may not be mean intensity alone but include some color-related parameter. Also, feature differences based on color, background, and shape criteria may also need to be developed. Furthermore, the discrimination of mixed textures (textures with more than one primitive) will have to be addressed. Finally, a model for stereo discrimination may also be developed.

Third, unambiguous methods for producing the kind of fuzzy map described above (which represents the real content of the map) need to be developed and tested. Compatibility tests aimed at evaluating where a new interpretation agrees with the existing maps and where it disagrees need to be developed. This will allow the use of forest maps within GIS without the database coherence problems which presently play havoc in the map update process.

Finally, it should be recognized that, although this work has been focused specifically on the problems of forest map-

ping and photointerpretation of forest stands, the main ideas touching the evaluation of local context, the measurement of boundary error, the relationship between boundary error and texture features, and the production of fuzzy content maps are probably applicable to almost any domain where photointerpretation is used. Hence, the mapping of soils, coastlines, crops, water courses, water sediments, geological features, snowfields, etc., may all benefit from this kind of error analysis. The interpretation of noisy imagery such as radar is also likely to profit, as is, indeed, the interpretation of the results of more automated image analysis techniques such as are widely used in remote sensing. And any domain which requires the long term coherence of a spatial database based on an error-prone information extraction process may benefit from this work.

Acknowledgments

This work was funded directly by the Association des industries forestières du Québec and the Natural Sciences and Engineering Research Council of Canada through the establishment of an Industrial Chair in Geomatics Applied to Forestry. Both authors would like to express gratitude to our colleague Chris Gold for his important contributions to the ideas which formed the basis of this study. We also appreciate the extensive and helpful comments made by the anonymous reviewers.

References

- Altman, D., 1992. Inexact spatial reasoning, *Proceedings of GIS'92*, Vancouver, B.C., Section D3, 9 p.
- Aubert, E., G. Edwards, and K.E. Lowell, 1994. Quantification des erreurs de frontières en photo-interprétation forestière, *Canadian Conference on GIS* (in press).
- Beck, J., 1966. Perceptual grouping produced by changes in orientation and shape, *Science*, 154:538-540.
- Beck, J., A. Sutter, and R. Ivry, 1987. Spatial frequency channels and perceptual grouping in texture segregation, *Computer Vision, Graphics and Image Processing*, 37:299-325.
- Bergen, J.R., 1991. Theories of visual texture perception, *Spatial Vision*, 10:114-134.
- Biging, G.S., R.G. Congalton, and E.C. Murphy, 1992. A comparison of photointerpretation and ground measurements of forest structure, *Proceedings of the ASPRS Annual Meeting*, Baltimore, Maryland, 3:6-15.
- Blakemore, M., 1984. Generalization and error in spatial databases, *Cartographica*, 21:131-139.
- Burrough, P.A., 1989. Fuzzy mathematical methods for soil survey and land evaluation, *Journal of Soil Science*, 40:477-492.
- Caelli, T.M., 1985. Three processing characteristics of visual texture segmentation, *Spatial Vision*, 1:19-30.
- , 1986. Three processing characteristics of texture discrimination, *Proceedings of Vision Interface '86*, pp. 343-348.
- Chrisman, N.R., 1982. A theory of cartographic error and its measurement in digital databases, *Proceedings of Auto-Carto 5*, Crystal City, Virginia, pp. 159-168.
- , 1987. The accuracy of map overlays: a reassessment, *Landscape and Urban Planning*, 14:427-439.
- , 1991. The error component in spatial data, *Geographical Information Systems* (D.J. Maguire, M.F. Goodchild, and D.W. Rhind, editors), Longman, U.K., pp. 164-174.
- Chrisman, N., and M. Lester, 1991. A diagnostic test for error in categorical maps, *Proceedings of Auto-Carto 10*, Baltimore, Maryland, pp. 330-348.
- Crain, I.K., P. Gong, M.A. Chapman, S. Lam, J. Alai, and M. Hoogstraat, 1993. Implementation considerations for uncertainty management in an ecologically-oriented GIS, *Proceedings of GIS'93*, Vancouver, B.C., pp. 167-172.
- Dick, R.C., and G.A. Jordan, 1990. GIS activity in Canadian forestry, *Forest Management and Geographic Information Systems*, 1: 144-176.
- Dougenik, J., 1980. Whirlpool: A geometric processor for polygon coverage data, *Proceedings AUTO-CARTO IV*, 2:304-311.
- Dunn, R., A.R. Harrison, and J.C. White, 1990. Positional accuracy and measurement error in digital databases of land use: An empirical study, *International Journal of Geographical Information Systems*, 4:385-398.
- Dutton, G., 1992. Handling positional uncertainty in spatial databases, *Proceedings of the Fifth International Symposium on Spatial Data Handling*, Charleston, South Carolina, pp. 460-469.
- Edwards, G., 1994. Characterising and maintaining polygons with fuzzy boundaries in geographic information systems, *Proceedings of the 6th Symposium on Spatial Data Handling* (submitted).
- Foody, G.M., 1992. On the compensation for chance agreement in image classification accuracy assessment, *Photogrammetric Engineering & Remote Sensing*, 58:1459-1460.
- Gong, P., and J. Chen, 1992. Boundary uncertainties in digitized maps 1: Some possible determination methods, *Proceedings of GIS/LIS '92*, pp. 274-281.
- Goodchild, M.F., 1977. Statistical aspects of the polygon overlay problem, *Harvard Papers on Geographical Information Systems*, Volume 6 (G. Dutton, editor), Addison Wesley, Reading, Massachusetts, pp. 1-22.
- , 1989. Preface, *Accuracy of Spatial Databases* (M. Goodchild and S. Gopal, editors), Taylor and Francis, New York, pp. xi-xv.
- Goodchild, M.F., and M.-H. Wang, 1988. Modelling error in raster-based spatial data, *Proceedings of the 3rd International Symposium on Spatial Data Handling*, Sydney, Australia, pp. 97-106.
- Haralick, R.M., 1979. Statistical and structural approaches to textures, *Proceedings IEEE*, 67:786-804.
- Haralick, R.M., K. Shanmugam, and I. Dinstein, 1973. Textural features for image classification, *IEEE Transactions on Systems, Man and Cybernetics*, 3:610-621.
- Julesz, B., 1962. Visual pattern discrimination, *IRE Transactions on Information Theory*, 8:84-92.
- , 1981. Textons, the elements of texture perception and their interaction, *Nature*, 290:91-97.
- Julesz, B., H.L. Frisch, E.N. Gilbert, and L.A. Shepp, 1973. Inability of humans to discriminate between visual textures that agree in second-order statistics - revisited, *Perception*, 2:391-405.
- Langran, G., 1992. *Time in Geographic Information Systems*, Taylor and Francis.
- Langran, G., and N.R. Chrisman, 1988. A framework for temporal geographic information, *Cartographica*, 25(3):1-14.
- Lowell, K.E., C.M. Gold, and G. Edwards, 1992. The next generation of digital spatial technologies: Error utilization, thematic map and remote sensing integration, spatial operators, and data structures, *Proceedings of GIS'92*, Vancouver, B.C., 6 p.
- Lunetta, R.S., R.G. Congalton, L.K. Fenstermaker, J.R. Jensen, K.C. McGwire, and L.R. Tinney, 1991. Remote sensing and geographic information system data integration: Error sources and research issues, *Photogrammetric Engineering & Remote Sensing*, 57(6):677-687.
- Nantel, J., 1993. A new and improved digitizing method based on the Thiessen (Voronoi) algorithm, *Proceedings of the Sixth Annual Genasys International Users Conference*, Fort Collins, Colorado, pp. 12-25.
- Pullar, D., 1991. Spatial overlay with inexact numerical data, *Proceedings of AutoCarto 10*, 6:313-329.
- Reed, T.R., and H. Wechsler, 1990. Segmentation of textured images and gestalt organisation using spatial/spatial-frequency representations, *IEEE Transactions on Pattern Analysis and Machine Intelligence*, 12(1):1-12.
- Rosenfeld, A., and M. Thurston, 1971. Edge and curve detection for visual scene analysis, *IEEE Transactions on Computers*, C-20: 562-569.
- Rosenfeld, G.H., and K. Fitzpatrick-Lins, 1986. A coefficient of agreement as a measurement of thematic classification accuracy, *Photogrammetric Engineering & Remote Sensing*, 52:223-227.

- Serra, J., 1982. *Image Analysis and Mathematical Morphology*, Academic Press, London.
- Story, M., and R. Congalton, 1986. Accuracy assessment: A user's perspective, *Photogrammetric Engineering & Remote Sensing*, 52(3):397-399.
- Tobler, W.R., 1969. Geographic filters and their inverses, *Geographical Analysis*, 1(3):234-253.
- Tomlinson, R.F., 1987. Current and potential uses of geographical information systems, the North American experience, *International Journal of Geographical Information Systems*, 1:203-218.
- Wertheimer, M., 1958. Principles of perceptual organization, *Readings in Perception*, (David C. Beardslee and Michael Wertheimer, editors), Van Nostrand Inc., New York, pp. 115-135.
- Wilson, R., and G.H. Granlund, 1984. The uncertainty principle in image processing, *IEEE Transactions on Pattern Analysis and Machine Intelligence*, 6(6):758-767.
- Zadeh, L.A., 1965. Fuzzy sets, *Information and Control*, 8:338.
- Zhang, G., and J. Tulip, 1990. An algorithm for the avoidance of sliver polygons and clusters of points in spatial overlay, *Proceedings of the 4th International Symposium on Spatial Data Handling*, pp. 141-150.

(Received 1 October 1993; revised and accepted 18 July 1994; revised 7 April 1995)

Forthcoming Articles

Articles listed in the April Forthcoming Articles are those scheduled through July 1996 only.

- M.J. Barnsley and S.L. Barr*, Inferring Urban Land Use from Satellite Sensor Images Using Kernel-Based Spatial Re-Classification.
- Ling Bian and Eric West*, GIS Modeling of Elk Calving Habitat in a Prairie Environment with Statistics.
- Lithologic Mapping of the Ice River Alkaline Complex, British Columbia, Canada, Using AVIRIS Data.
- Eduardo Brondizio, Emilio Moran, Paul Mausel, and You Wu*, Land Cover in the Amazon Estuary: Linking of Thematic Mapper with Botanical and Historical Data.
- B.H.C. Cheng, R.H. Bourdeau, and B.C. Pijanowski*, A Regional Information System for Environmental Data Analysis.
- John W. Dunham and Kevin P. Price*, Comparison of Nadir and Off-Nadir Multispectral Response Patterns for Six Tallgrass Prairie Treatments in Eastern Kansas.
- Giles M. Foody*, Relating the Land-Cover Composition of Mixed Pixels to Artificial Neural Network Classification Output.
- Mark Gahegan and Julien Flack*, A Model to Support the Integration of Image Understanding Techniques within a GIS.
- Jay Gao and Stephen M. O'Leary*, The Role of Spatial Resolution in Quantifying Suspended Sediment Concentration from Airborne Remotely Sensed Data.
- P. Gong*, Integrated Analysis of Spatial Data from Multiple Sources: Using Evidential Reasoning and Artificial Neural Network Techniques for Geological Mapping.
- Qizhong Guo and Norbert P. Psuty*, Flood-Tide Deltaic Wetlands: Detection of Their Sequential Spatial Evolution.
- N.G. Kardoulas, A.C. Bird, and A.I. Lawan*, Geometric Correction of SPOT and Landsat Imagery: A Comparison of Map and GPS Derived Control Points.
- Arnon Karnieli, Amnon Meisels, Leonid Fisher, and Yaacov Arkin*, Automatic Extraction and Evaluation of Geological Linear Features from Digital Remote Sensing Data Using a Hough Transform.
- Eric F. Lambin*, Change Detection at Multiple Temporal Scales: Seasonal and Annual Variations in Landscape Variables.
- Liang-Hwei Lee and Tsu-Tse Su*, Vision-Based Image Processing of Digitized Cadastral Maps.
- Kenneth C. McGwire*, Cross-Validated Assessment of Geometric Accuracy.
- Elijah W. Ramsey III and John R. Jensen*, Remote Sensing of Mangrove Wetlands: Relating Canopy Spectra to Site-Specific Data.
- Joel D. Schlager and Carlton M. Newton*, A GIS-Based Statistical Method to Analyze Spatial Change.
- Andrew K. Skidmore, Fional Watford, Paisan Luckananurug, and P. J. Ryan*, An Operational GIS Expert System for Mapping Forest Soils.
- M.D. Tomer, J.L. Anderson, and J.A. Lamb*, Assessing Corn Yield and Nitrogen Uptake Variability with Digitized Aerial Infrared Photographs.
- E. Lynn Usery*, A Feature-Based Geographic Information System Model.
- Jim Vrabel*, Multispectral Imagery Band Sharpening Study.
- James D. Wickham, Robert V. O'Neill, Kurt H. Ritters, Timothy G. Wade, and K. Bruce Jones*, Sensitivity of Selected Landscape Pattern Metrics to Land-Cover Misclassification and Differences in Land-Cover Composition.
- Eric A. Williams and Dennis E. Jelinski*, On Using the NOAA AVHRR "Experimental Calibrated Biweekly Global Vegetation Index."

June 1996 Special Issue on Softcopy Photogrammetry

- O. Kölbl and Bach*, Tone Reproduction of Photographic Scanners.
- Eugene E. Derenyi*, The Digital Transferscope.
- Weiyang Zhou, Robert H. Brock, and Paul F. Hopkins*, A Digital System for Surface Reconstruction.
- T. Ch. Massesware Rao, K. Venugopala Rao, A. Ravi Kumar, D.P. Rao, and B.L. Deekshatula*, Digital Terrain Model (DTM) from Indian Remote Sensing (IRS) Satellite Data from the Overlap Area of Two Adjacent Paths Using Digital Photogrammetric Techniques.
- Charles K. Toth and Amnon Krupnik*, Concept, Implementation, and Results of an Automatic Aerotriangulation System.
- Peggy Agouris and Toni Schenk*, Automated Aerotriangulation Using Multiple Image Multipoint Matching.
- Emmanuel P. Baltsavias*, Digital Ortho-Images: A Powerful Tool for the Extraction of Spatial- and Geo-Information.
- Kurt Novak and Fayez S. Shahin*, A Comparison of Two Image Compression Techniques for Softcopy Photogrammetry.